

Available online at www.sciencedirect.com

ScienceDirect

Biomedical Journal

journal homepage: www.elsevier.com/locate/bj

Original Article

Glycolytic metabolism and activation of Na^+ pumping contribute to extracellular acidification in the central clock of the suprachiasmatic nucleus: Differential glucose sensitivity and utilization between oxidative and non-oxidative glycolytic pathways

Hsin-Yi Lin ^a, Rong-Chi Huang ^{a,b,c,*}^a Department of Physiology and Pharmacology, College of Medicine, Chang Gung University, Taoyuan, Taiwan^b Healthy Aging Research Center, Chang Gung University, Taoyuan, Taiwan^c Neuroscience Research Center, Chang Gung Memorial Hospital at Linkou, Taoyuan, Taiwan

ARTICLE INFO

Article history:

Received 3 November 2020

Accepted 7 February 2021

Available online 12 February 2021

Keywords:

 Na^+/K^+ -ATPase

pH

Metabolism

Glycolysis

Suprachiasmatic nucleus

ABSTRACT

Background: The central clock of the suprachiasmatic nucleus (SCN) controls the metabolism of glucose and is sensitive to glucose shortage. However, it is only beginning to be understood how metabolic signals such as glucose availability regulate the SCN physiology. We previously showed that the ATP-sensitive K^+ channel plays a glucose-sensing role in regulating SCN neuronal firing at times of glucose shortage. Nevertheless, it is unknown whether the energy-demanding Na^+/K^+ -ATPase (NKA) is also sensitive to glucose availability. Furthermore, we recently showed that the metabolically active SCN constantly extrudes H^+ to acidify extracellular pH (pHe). This study investigated whether the standing acidification is associated with Na^+ pumping activity, energy metabolism, and glucose utilization, and whether glycolysis- and mitochondria-fueled NKAs may be differentially sensitive to glucose shortage.

Methods: Double-barreled pH-selective microelectrodes were used to determine the pHe in the SCN in hypothalamic slices.

Results: NKA inhibition with K^+ -free (0-K^+) solution rapidly and reversibly alkalinized the pHe, an effect abolished by ouabain. Mitochondrial inhibition with cyanide acidified the pHe but did not inhibit 0-K^+ -induced alkalinization. Glycolytic inhibition with iodoacetate alkalinized the pHe, completely blocked cyanide-induced acidification, and nearly completely blocked 0-K^+ -induced alkalinization. The results indicate that glycolytic metabolism and activation of Na^+ pumping contribute to the standing acidification. Glucoprivation also alkalinized the pHe, nearly completely eliminated cyanide-induced acidification, but only partially reduced 0-K^+ -induced alkalinization. In contrast, hypoglycemia preferentially and partially blocked

* Corresponding author. Department of Physiology and Pharmacology, College of Medicine, Chang Gung University, 259, Wenhua 1st Rd., Gueishan, Taoyuan 333, Taiwan.

E-mail address: rongchi@mail.cgu.edu.tw (R.-C. Huang).

Peer review under responsibility of Chang Gung University.

<https://doi.org/10.1016/j.bj.2021.02.004>

2319-4170/© 2021 Chang Gung University. Publishing services by Elsevier B.V. This is an open access article under the CC BY-NC-ND license (<http://creativecommons.org/licenses/by-nc-nd/4.0/>).

cyanide-induced acidification. The result indicates sensitivity to glucose shortage for the mitochondria-associated oxidative glycolytic pathway.

Conclusion: Glycolytic metabolism and activation of glycolysis-fueled NKA Na^+ pumping activity contribute to the standing acidification in the SCN. Furthermore, the oxidative and non-oxidative glycolytic pathways differ in their glucose sensitivity and utilization, with the oxidative glycolytic pathway susceptible to glucose shortage, and the non-oxidative glycolytic pathway able to maintain Na^+ pumping even in glucoprivation.

At a glance commentary

Scientific background on the subject

The SCN central clock is metabolically active to extrude H^+ to acidify extracellular pH and is susceptible to glucose shortage. We investigated whether the standing acidification is associated with Na^+ pumping activity, energy metabolism, and glucose utilization, and whether glycolysis- and mitochondria-fueled Na^+/K^+ -ATPase may be differentially sensitive to glucose shortage.

What this study adds to the field

Glycolytic metabolism and activation of glycolysis-fueled Na^+/K^+ -ATPase Na^+ pumping activity contribute to the standing acidification in the SCN. The oxidative and non-oxidative glycolytic pathways differ in glucose sensitivity and utilization, with the oxidative pathway susceptible to glucose shortage, and the non-oxidative pathway able to maintain Na^+ pumping even in glucoprivation.

Circadian clock and energy metabolism interact intimately with each other [1]. In mammals, the central clock in the hypothalamic suprachiasmatic nucleus (SCN) controls the circadian rhythm of physiology and metabolism [2]. The SCN clock exhibits diurnal rhythms in metabolic activity, with higher 2-deoxyglucose uptake [3,4], cytochrome oxidase activity [5], and Na^+/K^+ -ATPase (NKA) activity [6] during the day than at night. Multiple lines of evidence indicate that the SCN actively controls the metabolism of glucose, and the availability of which then feedbacks to act on the SCN to alter its circadian phase and photic entrainment to external light [7]. Specifically, insulin- or fasting-induced hypoglycemia has been shown to attenuate light-induced phase shifts at night in mice [8]. However, it is only beginning to be understood how energy metabolism regulates the SCN. Recently we found that the ATP-sensitive K^+ (K_{ATP}) channel plays a glucose-sensing role in regulating SCN neuronal firing at times of glucose shortage [9].

On the other hand, the electrogenic and energy-demanding nature of NKA also suggests a role in the metabolic regulation of excitability and ionic homeostasis in the SCN neurons [10–12]. In particular, the diurnal increase in 2-deoxyglucose uptake and cytochrome oxidase activity, which reflect respectively the glycolytic flux and mitochondrial respiration [13], suggests that rate of both glycolysis and oxidative phosphorylation is higher

during the day in the SCN. Together these observations may be taken to suggest a diurnal increase in glucose uptake as well as mitochondrial respiration to meet high energy demand for NKA Na^+ pumping activity. Nevertheless, in the rat SCN neurons NKA is fuelled by energy derived from both glycolysis and oxidative phosphorylation [11]. Since neuronal energy for supporting Na^+ pumping is mostly produced by oxidative phosphorylation [14], the presence of glycolysis-fueled NKA in the SCN neurons suggests a particular role and may sense and utilize glucose in a way different from the mitochondria-fueled NKA.

ATP hydrolysis, in particular when coupled with glycolysis, constantly produces H^+ [15,16], which could cause extracellular acidifications via multiple acid extrusion pathways [17]. We recently used double-barreled pH-selective microelectrodes to demonstrate a more acidic extracellular pH (pHe) in the SCN than the adjacent extra-SCN areas in hypothalamic slices [18], a result most likely due to the higher density packing of small SCN cells as well as higher level of metabolic activity than extra-SCN areas [4]. The maximum acidification at the center of 300- μm hypothalamic slices amounts to ~ 0.3 pH units when superfused with 10 mM HEPES-buffered solution at pH 7.4, and is partly mediated by H^+ extrusion via the constitutively active Na^+/H^+ -exchanger NHE1, which by doing so maintains a more alkaline intracellular pH to regulate particularly nimodipine-sensitive $[\text{Ca}^{2+}]_i$ in the soma [18].

As Na^+ pumping by NKA is considered the single most important energy consumer, it may contribute to the standing extracellular acidification in the SCN. In this study, we used double-barreled pH-selective microelectrodes to determine the pHe shifts associated with Na^+ pumping, energy metabolism, and glucose utilization in the rat SCN, and also investigated whether glycolysis- and mitochondria-fueled NKAs may be differentially sensitive to glucose shortage. Our results indicated that glycolytic metabolism and particularly glycolytic activation of Na^+ pumping contributes to the standing acidification in the SCN. Furthermore, our results revealed differences in glucose sensitivity and utilization between oxidative and non-oxidative glycolytic pathways, with the mitochondria-associated oxidative glycolytic pathway susceptible to glucose shortage, and the non-oxidative glycolytic pathway able to maintain Na^+ pumping at times of glucose shortage.

Material and methods

Hypothalamic brain slices

All experiments were carried out according to procedures approved by the Institutional Animal Care and Use Committee

of Chang Gung University. Sprague–Dawley rats of either sex (18–24 days old) were kept in a temperature-controlled room under a 12:12 light:dark cycle (light on 0700–1900 h). Lights-on was designated Zeitgeber time (ZT) 0. For daytime (ZT 4–11) and nighttime (ZT 13–20) recordings, the animal was killed at ZT 2 and ZT 10, respectively. Hypothalamic brain slices were made as described previously [18]. An animal was carefully restrained by hand to reduce stress and killed by decapitation using a small rodent guillotine without anesthesia, and the brain was put in an ice-cold artificial cerebrospinal fluid (ACSF) bubbled with 95% O₂–5% CO₂ or HEPES-buffered incubation solution bubbled with 100% O₂. The ACSF contained (in mM): 125 NaCl, 3.5 KCl, 2 CaCl₂, 1.5 MgCl₂, 26 NaHCO₃, 1.2 NaH₂PO₄, 10 glucose. A coronal slice (300 μm) containing the SCN and the optic chiasm was cut with a DSK microslicer (Ted Pella, Redding, CA, USA), incubated at room temperature (22–25 °C) for at least one hour in the incubation solution, which contained (in mM): 140 NaCl, 3.5 KCl, 2 CaCl₂, 1.5 MgCl₂, 10 glucose, 10 HEPES, pH 7.4, bubbled with 100% O₂, and was then transferred to a custom-made submerged-type recording chamber superfused with recording solution at a flow rate of 0.6–0.7 ml/min.

Extracellular pH measurements in hypothalamic slices

Extracellular pH in the SCN was measured with double-barreled pH-selective microelectrodes based on established methods [19,20] and was carried out as described previously [18]. The microelectrodes were pulled from double-barreled borosilicate glass capillaries with filament (2BF100-50-10, Sutter, Novato, CA, USA) with a vertical pipette puller (PE-21, Narishige, Japan). The tips were broken to a diameter of ~10 μm. The pH-selective barrel was selectively silanized with N,N-dimethyltrimethylsilylamine (Fluka 41,716, Sigma–Aldrich, St Louis, MO, USA) according to a modified method [21]. The reference and pH-selective barrels were backfilled with a solution containing (in mM): 100 NaCl, 20 HEPES, 10 NaOH, pH 7.4. Positive pressure was applied to the back of pH-selective barrel to ensure a good backfilling. A column of hydrogen ionophore I-cocktail A (Fluka 95,291; Sigma–Aldrich, St Louis, MO, USA) was then drawn into the tip of pH-selective barrel with or without suction. The electrode was calibrated before each experiment in a series of standard solutions [see Fig. 1 of ref. [18]]. The resistance of the pH-selective barrel was 5–10 GΩ, whereas the reference barrel had a resistance between 20 and 50 MΩ. All recordings were made with a Duo 773 Electrometer (World Precision Instruments, Sarasota, FL, USA) at room temperature (22–25 °C), with the signal low-pass filtered at 1 kHz and digitized online at 2 kHz with a PowerLab 4/30 (ADInstruments, Dunedin, New Zealand). All experiments were performed in HEPES-buffered solution that contains (in mM): 140 NaCl, 3.5 KCl, 2 CaCl₂, 1.5 MgCl₂, 10 HEPES, 10 glucose, pH 7.4.

Data were analyzed and plotted with custom-made programs written in Visual Basic 6.0 and the commercial software GraphPad PRISM (GraphPad Software, San Diego, CA, USA). Data were given as means ± SEM and analyzed with Student's t-test or paired t-test.

Drugs

Stock solutions of amiloride and DIDS (500 mM in DMSO) was stored at –20 °C, and was diluted at least 1000 times to reach desired final concentrations. Amiloride was purchased from Sigma–Aldrich (St Louis, MO, USA). K⁺-free solutions were prepared with omission of extracellular K⁺, glucose-free solutions with omission of glucose, and 0.5 mM glucose solutions with addition of 0.5 mM glucose. Ouabain, sodium cyanide (NaCN), and iodoacetate were directly added to the bath to achieve the final concentrations. These chemicals were purchased from Sigma–Aldrich. All solutions were adjusted to pH 7.4 before use.

Results

The effects of ouabain and K⁺-free solution on the pHe

NKA utilizes energy derived from ATP hydrolysis, to transport three Na⁺ ions out of the cell in exchange for two K⁺ ions into the cell, and releases as byproducts ADP, phosphate, and H⁺. To determine whether Na⁺ pumping produces H⁺ to contribute to the standing extracellular acidification, we investigated the effect of NKA blockers, the cardiac glycoside ouabain and K⁺-free (0-K⁺) solution, on the resting pHe in the SCN. Both ouabain and K⁺-free solution have been used previously to determine the effects of NKA blockade on membrane excitability, [Na⁺]_i, and [Ca²⁺]_i in the rat SCN neurons [10,12,22]. The result showed that bath application of 5 mM (or 1 mM) ouabain generally increased the pHe to reach a peak value in the first 5–10 min and then began to decrease toward the basal level, a result reminiscent of ouabain-induced biphasic change in [Ca²⁺]_i in the SCN cells [12]. Fig. 1A shows one such result to indicate the alkalinizing effect of 5 mM ouabain on the pHe. On average, the extracellular acidification in the center of the SCN was 0.28 ± 0.02 pH units (n = 6 slices), confirming our previous observation [18], and 5 mM ouabain increased the pHe by 0.17 ± 0.03 pH units (n = 6 slices). Note that the effect of ouabain on the pHe was virtually irreversible, as has been previously demonstrated in its effect on [Na⁺]_i in the SCN cells [12].

Contrary to the poorly reversible effect of ouabain, the effect of K⁺-free solution on NKA was rapid and reversible for the SCN neurons in reduced slice preparations [10,11]. We thus also used K⁺-free solution to determine its effect on the pHe. It should be reminded that in the hypothalamic slice the extracellular K⁺ concentration may not be clamped to zero K⁺ due to constant efflux of K⁺ from cells. Fig. 1B shows an experiment to indicate the effect of zero K⁺ on the pHe in the absence and then the presence of 5 mM ouabain (left panel). Removal of external K⁺ caused a rapid alkaline shift that reached a peak in the first 2–3 min and readmission of 3.5 mM K⁺ rapidly returned the pHe followed by a slower acidification (marked by arrow). The waveform of 0-K⁺-evoked pHe shifts is reminiscent of 0-K⁺-evoked changes in membrane potential [see Fig. 1B of ref. [11]] and [Ca²⁺]_i [see

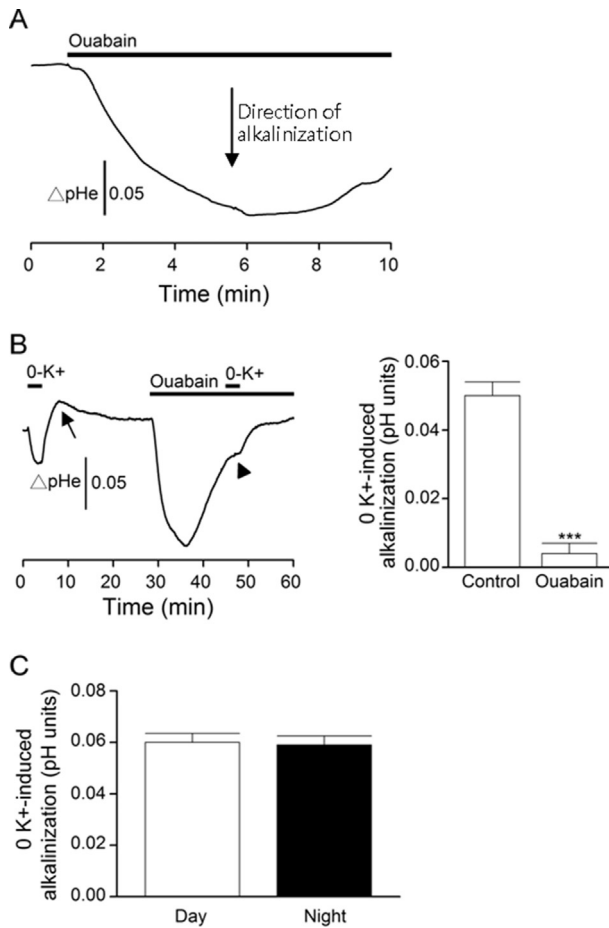


Fig. 1 Na⁺/K⁺-ATPase (NKA) activity contributes to the standing extracellular acidification. (A) Effect of 5 mM ouabain on the extracellular pH (pHe) from a representative experiment. (B) Left: A representative result to show the effect of K⁺-free solution on the pHe in control and in 5 mM ouabain. Right: Statistics comparing the average amplitude of 0-K⁺-induced alkalization in control and in 5 mM ouabain. ****p* < 0.001. (C) Statistics showing a similar amplitude of 0-K⁺-induced alkalization recorded between day (ZT 4–11) and night (ZT 13–21).

Fig. 1 of ref. [22]. The alkaline shift induced by K⁺-free solution was, however, ~3 times smaller than that by ouabain and was nearly completely eliminated (marked by arrow-head) in ouabain to block NKA, suggesting an incomplete blockade of NKA by K⁺-free solution. The incomplete blockade of NKA by K⁺-free solution was apparently due to non-zero concentration of K⁺ (~1–2 mM) in the extracellular space as measured with K⁺-selective electrodes (HY Lin and RC Huang, unpublished observations). On average, ouabain reduced the magnitude of 0-K⁺-induced alkalization from 0.050 ± 0.004 pH units (*n* = 6 slices) to 0.004 ± 0.003 pH units (*n* = 6 slices) (*p* = 0.0002, paired t-test) (right panel). Together, the results suggest that NKA Na⁺ pumping contributes to the standing extracellular acidification in the SCN.

We previously showed that the standing extracellular acidification is partly mediated by H⁺ extrusion via the Na⁺/H⁺-exchanger NHE1 [18]. To investigate whether NKA-

associated extracellular acidification is mediated by H⁺ extrusion via NHE1, we determined the effect of 100 μ M amiloride on the magnitude of 0-K⁺-evoked alkalization. The result showed little effect of amiloride on the magnitude of 0-K⁺-induced alkalization (HY Lin and RC Huang, unpublished observations), suggesting that mechanisms other than NHE1 may mediate the NKA-associated extracellular acidification. Indeed, our preliminary results showed that 500 μ M DIDS, an inhibitor of the SLC4 family of bicarbonate-transporters [23], partially blocked 0-K⁺-evoked alkalization (HY Lin and RC Huang, unpublished observations), suggesting an involvement of the bicarbonate transporter.

The magnitude of 0-K⁺-induced alkalization was similar between day (ZT 4–11) and night (ZT 13–20), the respective values being 0.060 ± 0.004 pH units (*n* = 29 slices) and 0.059 ± 0.004 pH units (*n* = 17 slices) (*p* = 0.87, Student's t-test) [Fig. 1C]. Note that the magnitude of the standing extracellular acidification was also similar between day and night [18]. Although the K⁺-free solution used in this study did not block NKA as effectively as ouabain, the virtually irreversible effect of ouabain on the pHe prevents us from using this drug to do repetitive applications as required in the following experiments. Thus we have used zero K⁺ to assess the NKA Na⁺ pumping activity, with occasional use of ouabain for comparison.

Cyanide effects

In the rat SCN neurons, NKA is fuelled by ATP derived from both glycolysis and oxidative phosphorylation, as demonstrated by the result that 0-K⁺-induced depolarization was incompletely blocked by mitochondrial inhibition with cyanide and completely blocked by glycolytic inhibition with iodoacetate [11]. To determine the contribution of mitochondria-fueled NKA to extracellular acidification, we studied 0-K⁺-induced alkalization in the absence and then the presence of 1 mM cyanide to block mitochondrial respiration [Fig. 2]. The result shows that cyanide inhibition of mitochondrial respiration markedly acidified the pHe [Fig. 2A, left panel]. On average, cyanide-induced acidification was 0.46 ± 0.09 pH units (*n* = 10 slices), and was similar between day (ZT 4–11) and night (ZT 13–20), with the respective values being 0.49 ± 0.14 pH units (*n* = 5 slices) and 0.43 ± 0.11 pH units (*n* = 5 slices) (*p* = 0.73, Student's t-test) (right panel). The cyanide-induced acidification was associated with glycolytic metabolism as will be presented later [see Figs. 3C and 5A]. Note the initial alkalization in response to the application of cyanide (marked by arrow). The cyanide-induced initial alkalization averaged 0.018 ± 0.003 pH units (*n* = 10 slices), and was similar in its amplitude between day and night, being 0.017 ± 0.003 pH units (*n* = 5 slices) at day and 0.019 ± 0.006 pH units (*n* = 5 slices) (*p* = 0.77, Student's t-test) at night. Cyanide-induced initial alkalization has been previously observed in cardiac Purkinje fiber [24–26] and attributed to increased hydrolysis of phosphocreatine and thus a drop in proton concentration [24].

While cyanide inhibition of mitochondrial respiration produced marked extracellular acidifications, it did not appear to inhibit 0-K⁺-induced alkalization [Fig. 2A, left panel]. Fig. 2B, left panel, superimposes 0-K⁺-induced alkalization recorded in control [trace a; from Fig. 2A], in cyanide (trace b), and after

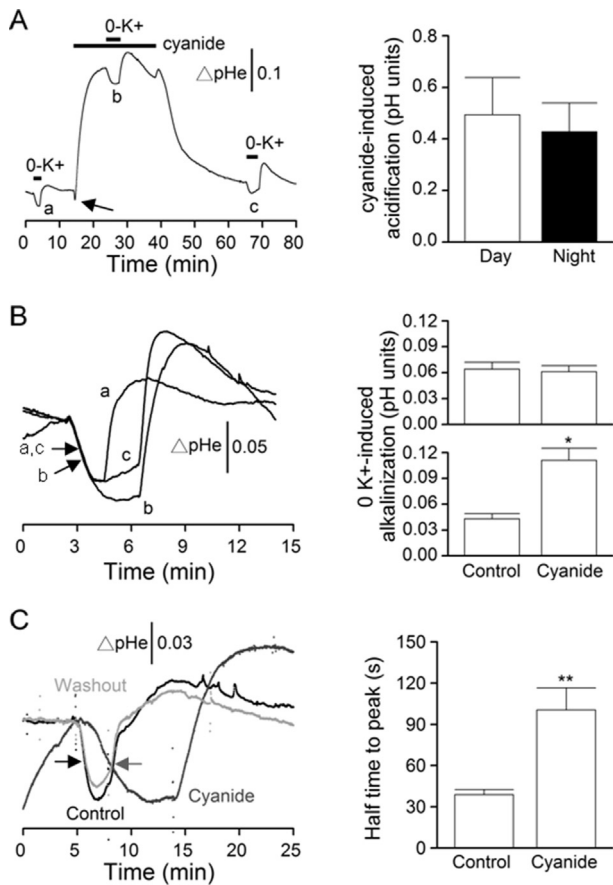


Fig. 2 Cyanide effects on the resting extracellular pH (pHe) and 0-K^+ -induced alkalinization. (A) A representative result showing the pHe response to K^+ -free solution in control (a), in 1 mM NaCN to block mitochondrial respiration (b), and after washout of NaCN (c). Note the cyanide-induced large acidification following an initial small alkalinization (marked by arrow) (left). Right: Statistics showing a similar magnitude of cyanide-induced acidification between day (ZT 4–11) and night (ZT 13–20). (B) Superimposition of the 0-K^+ responses (a, b, c; from a) indicating a reversible increase in the magnitude of 0-K^+ -induced alkalinization by cyanide (left). Note a moderate increase of $t_{1/2}$ (marked by arrows) by cyanide. Right: Statistics showing two different cyanide effects, a lack of effect (top) and an enhancing effect (bottom), on the magnitude of 0-K^+ -induced alkalinization recorded from two subgroups. * $p < 0.05$. (C) Superimposition of the 0-K^+ responses (control, cyanide, and washout) from another experiment to indicate a marked increase in $t_{1/2}$ by cyanide (marked by arrows) (left). Right: Statistics showing the average $t_{1/2}$ value of the 0-K^+ -induced alkalinization in control and in cyanide. Note a more than twofold increase in the $t_{1/2}$ value by cyanide. ** $p < 0.01$.

washout (trace c), showing that cyanide induced a reversible increase in the magnitude for this particular experiment. Cyanide also increased the half time ($t_{1/2}$, marked by arrows) to peak amplitude, from 32 s to 41 s. For a total of 10 experiments, cyanide statistically insignificantly increased the magnitude of 0-K^+ -induced alkalinization from 0.053 ± 0.006 pH units ($n = 10$

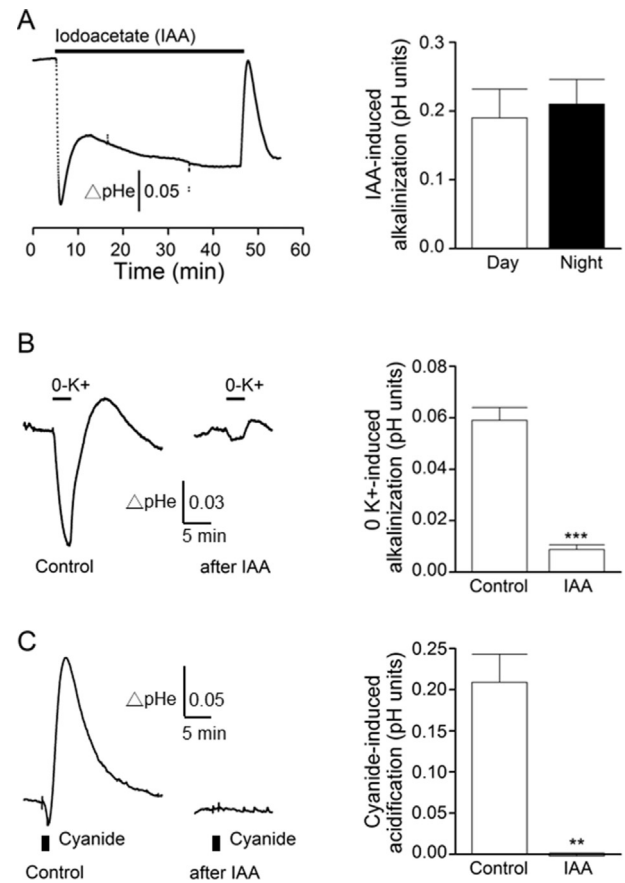


Fig. 3 Iodoacetate (IAA) effects on the resting extracellular pH (pHe), 0-K^+ -induced alkalinization, and cyanide-induced acidification. (A) A representative result showing the pHe response to glycolytic inhibition with 10 mM iodoacetate (left). Note the transient pHe responses to the wash-in and wash-out of the iodoacetate solution. Right: Statistics showing a similar magnitude of iodoacetate-induced alkalinization between day (ZT 4–11) and night (ZT 13–20). (B) A representative experiment to show a marked irreversible inhibition of 0-K^+ response after 30 min exposure to 10 mM iodoacetate (left). Right: Statistics showing the average amplitude of 0-K^+ -induced alkalinization in control and after 30 min exposure of iodoacetate. *** $p < 0.001$. (C) A representative experiment to show a complete block by iodoacetate of the cyanide response (left). Right: Statistics showing the average amplitude of cyanide-induced acidification in control and after 30 min exposure of iodoacetate. ** $p < 0.01$.

slices) to 0.086 ± 0.014 pH units ($n = 10$ slices) ($p = 0.069$, paired t -test). A closer inspection of the result, however, reveals two different responses to cyanide. In half of experiments (5 out of 10 slices) with cyanide altering the magnitude of 0-K^+ -induced alkalinization by less than 10%, the magnitude was similar in control and in cyanide, respectively, being 0.064 ± 0.008 pH units ($n = 5$ slices) and 0.061 ± 0.007 pH units ($n = 5$ slices) ($p = 0.47$, paired t -test) (top right panel). In the other half with cyanide increasing the magnitude of 0-K^+ -induced alkalinization by more than 10%, cyanide significantly increased the magnitude from 0.043 ± 0.006 pH units ($n = 5$ slices) to

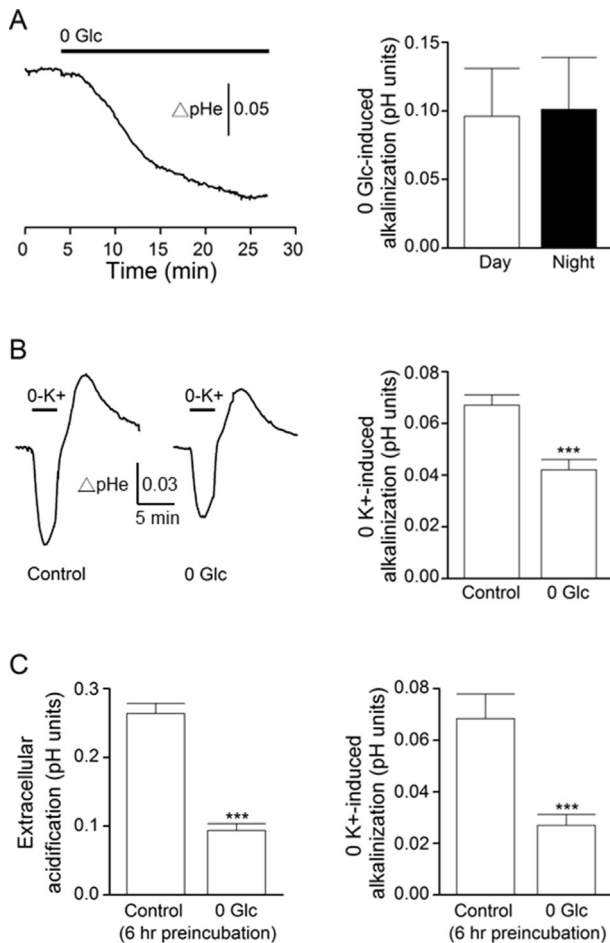


Fig. 4 Glucoprivation effects on the resting extracellular pH (pHe) and O-K⁺-induced alkalization. (A) A representative result showing the pHe response to the removal of external glucose (left). Right: Statistics showing a similar magnitude in the alkaline shift induced by glucose-free solution for ~30 min between day (ZT 7–11) and night (ZT 12–16). (B) A representative experiment to show the inhibition of O-K⁺-induced alkalization by glucose-free solution for ~45 min (left). Right: Statistics showing the average amplitude of O-K⁺-induced alkalization in control and after 30–60 min withdrawal of glucose. ****p* < 0.001. (C) Statistics showing the effect of prolonged (6–9 h) glucoprivation on the standing acidification (left) and the magnitude of O-K⁺-induced alkalization (right). ****p* < 0.001.

0.111 ± 0.023 pH units (*n* = 5 slices) (*p* = 0.039, paired *t*-test) (bottom right panel). The reason for the different responses to cyanide between the two subgroups is currently not known. Nevertheless, as extracellular acidification associated with NKA Na⁺ pumping appears to be mediated by glycolysis-fueled NKA [see Fig. 3], the result implies that mitochondrial inhibition enhances glycolytic activation of Na⁺ pumping in some but not in others.

Unlike a moderate increase in the *t*_{1/2} value by cyanide as shown in Fig. 2B, cyanide may markedly slow the rate of O-K⁺-induced alkalization to greatly increase the *t*_{1/2} value. Fig. 2C, left panel, shows one such result by superimposing the pHe response to K⁺-free solution before (black trace), during

(dark-grey trace), and after (grey trace) cyanide. For this particular experiment, cyanide had minimal effect on the amplitude, but markedly increased the *t*_{1/2} value from 32 s (marked by black arrow) to 104 s (marked by dark grey arrow). On average, cyanide increased the *t*_{1/2} value from 39 ± 4 s (*n* = 10 slices) to 101 ± 16 s (*n* = 10 slices) (*p* = 0.0035, paired *t*-test) [Fig. 2C, right panel]. Cyanide-induced increase in the buffering power such as phosphate has been shown to slow the rate of change in the pH response [24,26].

Iodoacetate effects

In contrast to mitochondrial inhibition with cyanide, which reversibly produced marked acidosis and might enhance O-K⁺-induced alkalization, glycolytic inhibition with iodoacetate irreversibly alkalinized the pHe and markedly blocked O-K⁺-induced alkalization [Fig. 3]. Fig. 3A shows the effect of 10 mM iodoacetate on the resting pHe from a representative experiment (left panel). As indicated, iodoacetate caused a rapid transient alkalization on top of a slower developing, sustained alkalization, and its washout produced only a rapid transient acidification without altering the sustained alkalization. Both the peak amplitudes of rapid transient pHe shifts were smaller with 2 mM iodoacetate (not shown), suggesting an origin of uncharged molecules (iodoacetic acid) entering and leaving the cells. Nevertheless, the steady-state alkalization at ~30 min into the application of 2 or 10 mM iodoacetate was similar, being 0.22 ± 0.05 pH units (*n* = 6 slices) and 0.19 ± 0.03 pH units (*n* = 9 slices) (*p* = 0.69, Student's *t*-test), respectively. Pooled together iodoacetate increased the pHe by 0.20 ± 0.03 pH units (*n* = 15 slices), compared to the standing acidification of 0.28 ± 0.03 pH units (*n* = 15 slices), suggesting that glycolytic metabolism contributes to the standing extracellular acidification in the SCN. Comparison of the iodoacetate responses recorded between day (ZT 4–11) and night (ZT 13–20) indicates a similar degree of iodoacetate-induced alkalization, the respective values being 0.19 ± 0.04 pH units (*n* = 6 slices) and 0.21 ± 0.04 pH units (*n* = 9 slices) (*p* = 0.74, Student's *t*-test) [Fig. 3A, right panel].

Fig. 3B shows the irreversible blockade by iodoacetate of O-K⁺-induced alkalization by comparing the pHe responses to K⁺-free solution before and after ~30 min of iodoacetate application (left panel). On average, the magnitude of O-K⁺-induced alkalization was reduced from 0.059 ± 0.005 pH units (*n* = 12 slices) in control to 0.009 ± 0.002 pH units (*n* = 12 slices) after iodoacetate (*p* < 0.001; paired *t*-test) (right panel). Similarly, the magnitude of ouabain-induced alkalization after iodoacetate treatment averaged 0.013 ± 0.011 pH units (*n* = 6 slices), ~10% of that determined in control (0.17 ± 0.03 pH units; *n* = 6 slices, Fig. 1A) (*p* = 0.0006; Student's *t*-test). Together the results indicate that glycolytic metabolism and activation of Na⁺ pumping contribute to the standing extracellular acidification in the SCN.

Importantly, iodoacetate also blocked cyanide-induced acidification [Fig. 3C]. The experiment was done by applying cyanide for 1 min to induce transient acidification. As indicated, cyanide-induced transient acidification was completely blocked after 30 min application of iodoacetate (left panel). On average, cyanide-induced acidification was reduced from 0.21 ± 0.03 pH units (*n* = 6 slices) in control to -0.002 ± 0.003 pH

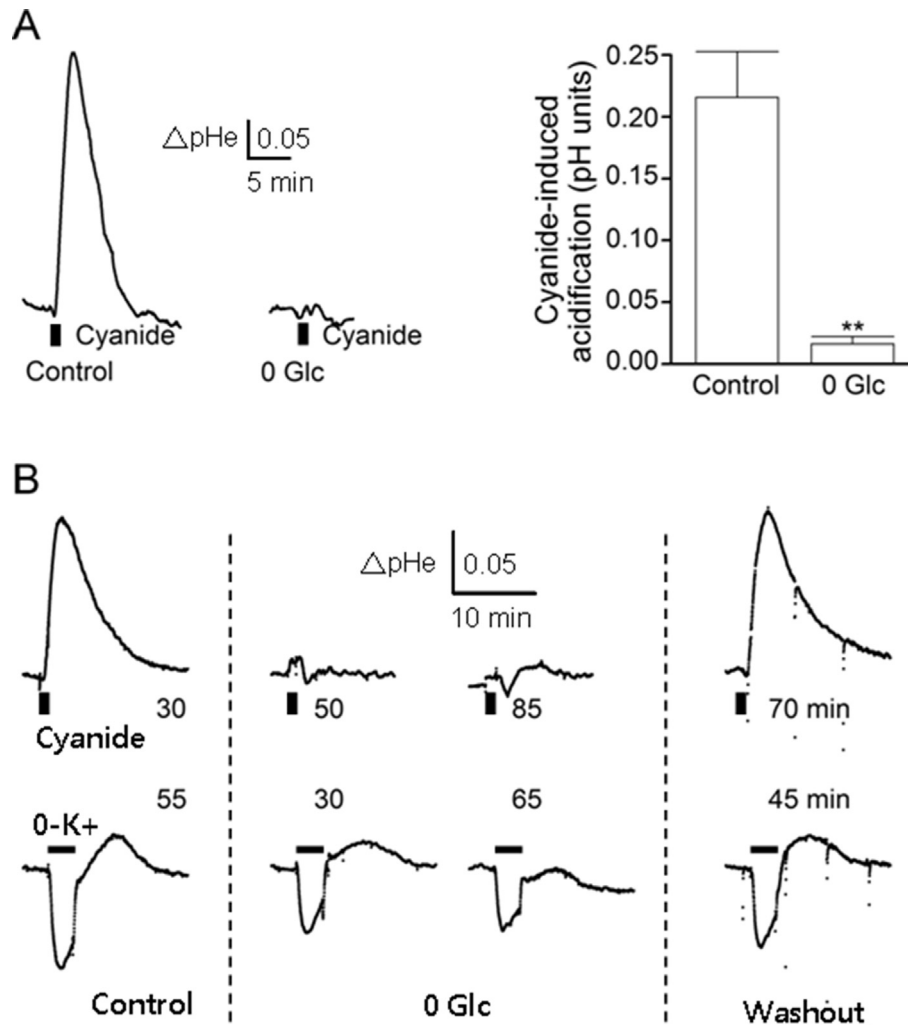


Fig. 5 Glucoprivation effects on cyanide-induced acidification. (A) A representative experiment to show the effect of glucoprivation on the cyanide-induced extracellular pH (pHe) transient (left). Note the complete block of the cyanide response by glucose withdrawal for ~30 min. Right, Statistics showing the average amplitude of cyanide-induced acidification in control and after 20–60 min withdrawal of glucose. $**p < 0.01$. (B) A representative result to demonstrate the differential effects of glucoprivation on cyanide-induced acidification and 0-K^+ -induced alkalization in the same slice. The number marks the time in min before (control), during (0-Glc), and after (washout) glucose withdrawal. Note the complete inhibition and full recovery of cyanide-induced acid shifts in response to glucose withdrawal and readmission of glucose, respectively. Similar results were from two other experiments.

units ($n = 6$ slices) ($p = 0.002$, paired t-test) after iodoacetate (right panel). The result indicates that the cyanide-induced acidification was also mediated by acid production associated with glycolytic metabolism.

Glucoprivation effects

The effect of glucose on the resting pHe and 0-K^+ -induced alkalization was determined by removing glucose from the superfusate [Fig. 4]. Glucose withdrawal increased the resting pHe with various length of delay to generally reach a steady state in between 20 and 60 min, and return to control (10 mM glucose) solution reacidified the pHe and may produce rebound acidification after more prolonged glucose withdrawal. Fig. 4A shows a representative result of pHe response to glucose-free solution (left panel). On average, zero glucose

(0-Glc) for 30 min produced an alkalization of 0.096 ± 0.026 pH units ($n = 10$ slices), with the standing acidification being 0.30 ± 0.01 pH units ($n = 10$ slices). The magnitude of 0-Glc-induced alkalization was similar between day (ZT 7–11) and night (ZT 12–16), respectively, being 0.091 ± 0.035 pH units ($n = 5$ slices) and 0.101 ± 0.038 pH units ($n = 5$ slices; $p = 0.85$, Student's t-test) (right panel).

Fig. 4B shows the pHe response to K^+ -free solution before and after ~45 min of glucose withdrawal (left panel), indicating only a partial inhibition of 0-K^+ -induced alkalization by glucose-free solution. On average, glucoprivation for 30–60 min only moderately reduced the magnitude of 0-K^+ -induced alkalization from 0.067 ± 0.004 pH units ($n = 9$ slices) to 0.042 ± 0.005 pH units ($n = 9$ slices) ($p = 0.0004$, paired t-test) (right panel). The moderate inhibition of 0-K^+ response by glucoprivation suggests the continuing metabolism to energize

glycolysis-fueled NKA Na^+ pumping in spite of the lack of exogenous glucose.

To further test this idea, we recorded the resting pHe and 0-K^+ -induced alkalinization after more prolonged (6–9 h) glucoprivation. Fig. 4C summarizes the results thus obtained from slices that have been incubated in control or glucose-free solution for at least 6 h. On average, the resting pHe after >6 h incubation in control and in glucose-free solution, respectively, were 0.26 ± 0.01 pH units ($n = 6$ slices) and 0.093 ± 0.010 pH units ($n = 11$ slices) ($p < 0.0001$, Student's *t*-test) (left panel), and the 0-K^+ -induced alkalinization, 0.068 ± 0.010 pH units ($n = 6$ slices) and 0.027 ± 0.004 pH units ($n = 11$ slices) ($p = 0.0004$, Student's *t*-test) (right panel). That there remains, albeit to smaller extents, the standing acidification and 0-K^+ -induced alkalinization even after prolonged glucoprivation for >6 h suggests the presence of energy reserve to support glycolytic metabolism, at least, to fuel Na^+ pumping activity.

In sharp contrast, glucoprivation appeared to completely block cyanide-induced acidification in most (5/6) slices in 20–60 min [Fig. 5]. Fig. 5A shows one such result (left panel). On average, glucoprivation markedly reduced cyanide-induced acidification from 0.22 ± 0.04 pH units ($n = 6$ slices) to 0.016 ± 0.006 pH units ($n = 6$ slices) ($p = 0.0058$, paired *t*-test) (right panel). Together with the result of Fig. 3C, the blockade of cyanide-induced acidification by glycolytic inhibition with iodoacetate or glucoprivation suggests a functional link between glycolysis and mitochondrial respiration. As oxidative phosphorylation is the main sink for protons [15], the cyanide-induced acid shift suggests a block of proton uptake by mitochondria and/or an increase in proton production by non-mitochondrial ATP hydrolysis [16].

Comparison of the effects of glucoprivation on the pHe responses to 0-K^+ [Fig. 4B] and cyanide [Fig. 5A] indicates that while glucoprivation could completely eliminate the cyanide response for as short as ~30 min [Fig. 5A], it only partially inhibited 0-K^+ response [Fig. 4B]. In other words, the pHe responses to cyanide and K^+ -free solution are differentially affected by glucoprivation. To better establish this fact, we compared the effects of glucoprivation on the pHe responses to cyanide and 0-K^+ in the same slices. Fig. 5B shows the result obtained from one such experiment. The number marks the time in min before (leftmost two panels), during (middle four panels), and after (rightmost two panels) glucose withdrawal. As indicated, for this particular experiment, cyanide-induced acidification was completely eliminated at ~50 min into glucose withdrawal, whereas 0-K^+ -induced alkalinization was only partially reduced. Together the result indicates differences in glucose utilization between the oxidative and non-oxidative glycolytic pathways. The abolition of cyanide, as opposed to 0-K^+ , response in glucose-free solution indicates the requirement for exogenous glucose to sustain mitochondria-associated, oxidative glycolytic metabolism, whereas the non-oxidative glycolytic metabolism can continue, albeit to a lesser extent, to provide energy for the glycolysis-fueled NKA.

Hypoglycemic effects

The reliance on exogenous glucose of cyanide, but not 0-K^+ , response suggests that cyanide response might be preferentially

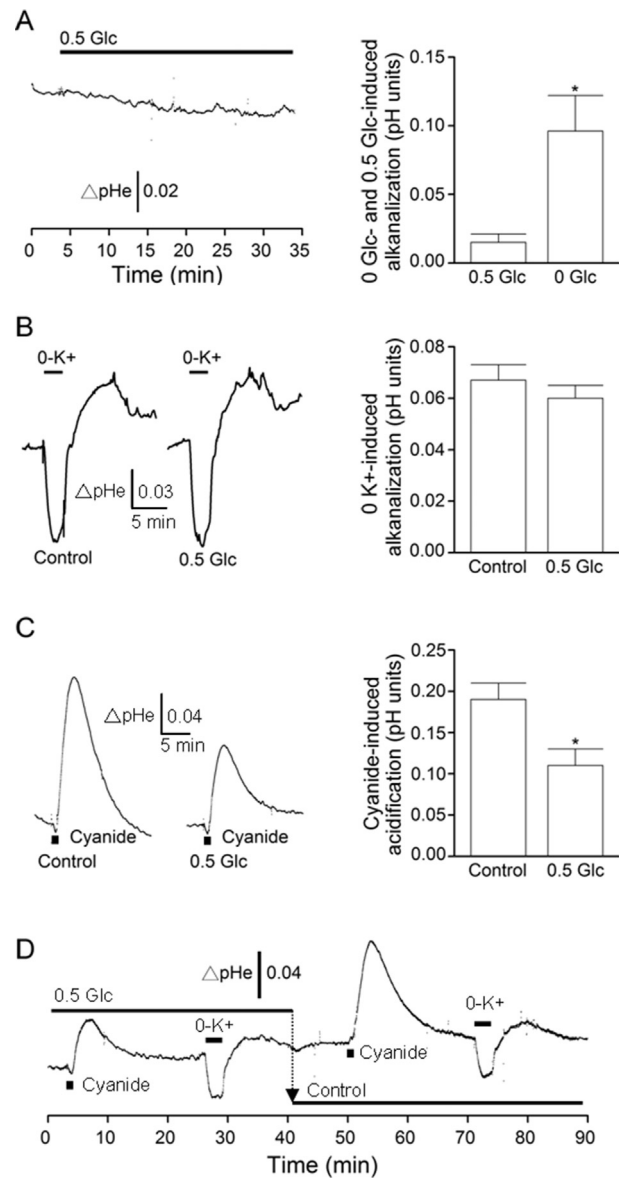


Fig. 6 Hypoglycemia (0.5 mM glucose) preferentially inhibits mitochondria-associated glycolysis. (A) Left: A representative experiment to show a small pHe response to the lowering of external glucose to 0.5 mM for 30 min. Right: Statistics showing the average amplitude of alkalinization induced by hypoglycemic and glucose-free solution (for 30 min). (B) A representative experiment to show the 0-K^+ -induced alkalinization in control and in 0.5 mM glucose solution for ~45 min (left). Right: Statistics showing a similar amplitude of 0-K^+ -induced alkalinization in control and after 30–60 min application of 0.5 mM glucose solution. (C) Left: Effect of 0.5 mM glucose on the cyanide-induced pHe transient from a representative experiment. Right: Statistics showing a marked reduction in the cyanide-induced acidification by 0.5 mM glucose for ~1 h. (D) A continuous recording trace (the same slice as in (C)) showing a full recovery of the cyanide response after return to control solution. * $p < 0.05$.

compromised by glucose shortage. This is indeed the case as demonstrated by the preferential inhibition of cyanide response

with hypoglycemic (0.5 mM glucose) solution [Fig. 6]. Fig. 6A shows a minimal effect of hypoglycemia on the resting pHe recorded from a representative slice (left panel). On average, hypoglycemia produced an alkalinization of 0.015 ± 0.006 pH units ($n = 6$ slices) in the first 30 min, significantly smaller than an alkalinization of 0.096 ± 0.026 pH units ($n = 10$ slices; $p = 0.033$, Student's *t*-test) induced by glucoprivation (right panel).

The magnitude of 0-K⁺-induced alkalinization was also not much altered by switching to hypoglycemic solution for ~45 min [Fig. 6B, left panel]. Note that in some experiments (2 out of 6 slices) the magnitude of 0-K⁺-induced alkalinization was slightly enhanced by 0.5 mM glucose. On average, hypoglycemia insignificantly reduced the magnitude from 0.067 ± 0.006 pH units ($n = 6$ slices) to 0.060 ± 0.005 pH units ($n = 6$ slices) ($p = 0.43$, paired *t*-test) [Fig. 6B, right panel].

In contrast to an insignificant effect on 0-K⁺-induced alkalinization, hypoglycemia markedly reduced cyanide-induced acidification as indicated by the result obtained from a representative slice [Fig. 6C, left panel]. On average, hypoglycemia reduced cyanide-induced acidification from 0.19 ± 0.02 pH units ($n = 6$ slices) to 0.11 ± 0.02 pH units ($n = 6$ slices) ($p = 0.013$, paired *t*-test) (right panel). The preferential inhibition by hypoglycemia of cyanide-induced acidification, as opposed to 0-K⁺-induced alkalinization, can also be clearly seen by the rapid, full recovery of cyanide response after returning to control solution [Fig. 6D], indicating that the mitochondria-associated, oxidative glycolytic pathway is sensitive to glucose shortage.

Discussion

The central clock in the SCN is metabolically active, constantly extruding H⁺, partly via the Na⁺/H⁺-exchanger NHE1, to create standing extracellular acidification in the SCN [18]. In this study we asked whether the standing acidification is associated with Na⁺ pumping activity, energy metabolism, and glucose utilization. The results show that glycolytic metabolism and, in particular, glycolytic activation of Na⁺ pumping contribute to the standing acidification in the SCN. We also asked whether glycolysis- and mitochondria-fueled NKAs may be differentially sensitive to glucose shortage. The results reveal differences in glucose sensitivity and utilization between the oxidative and non-oxidative glycolytic pathways. Specifically, the mitochondria-associated, oxidative glycolytic pathway is susceptible to glucose shortage, suggesting a role in metabolic regulation of the circadian clock. In contrast, the non-oxidative glycolytic pathway could continue to support Na⁺ pumping activity even in prolonged glucoprivation, suggesting an important role of glycolysis-fueled NKA at times of glucose shortage.

Glycolytic metabolism and activation of Na⁺ pumping contribute to the standing extracellular acidification in the SCN

Two principal observations lead us to conclude that glycolytic activation of Na⁺ pumping contributes to the standing

acidification in the SCN. First, the blockade of NKA with ouabain or K⁺-free solution produced alkaline shifts in the pHe. Second, 0-K⁺ (and ouabain)-induced alkalinization was abolished by metabolic inhibition of glycolysis but not mitochondrial respiration. Our unpublished results indicated that the acidification caused by the glycolysis-fueled NKA, however, is not mediated by H⁺ extrusion via NHE1, but rather is partly associated with DIDS-sensitive bicarbonate transporters. We have also used RT-PCR analysis to identify mRNAs for multiple members of the SLC family of bicarbonate transporters (HY Lin and RC Huang, unpublished observations). Further work is needed to better determine the acid extruders responsible for the extracellular acidification associated with glycolysis-fueled NKA Na⁺ pumping activity.

Our results also indicate an important contribution of glycolytic metabolism to the standing acidification in the SCN. First, glycolytic inhibition with iodoacetate, but not mitochondrial inhibition with cyanide, markedly alkalinized the pHe by ~0.2 pH units, compared to ~0.3 pH units of standing acidification. Second, glucoprivation also alkalinized the pHe by ~0.1 pH units. The results are consistent with the idea of H⁺ production by ATP hydrolysis, in particular when coupled with glycolysis [15,16].

On the other hand, cyanide inhibition of mitochondrial respiration produced marked extracellular acidosis, which was abolished by glycolytic inhibition with either iodoacetate or glucoprivation. The results suggest that the cyanide-evoked acidosis is associated with acids production along the oxidative glycolytic pathway. As oxidative phosphorylation is the main sink for protons [15], the cyanide-induced acid shifts suggest a block of proton uptake by mitochondria and/or an increase in proton production by non-mitochondrial ATP hydrolysis [16]. Indeed, the cyanide-enhanced 0-K⁺ response in approximately half of the experiments [Fig. 2B] is consistent with the idea that mitochondrial inhibition increases the glycolysis-fueled Na⁺ pumping activity, thereby increasing proton production. The underlying mechanism most likely involves cyanide inhibition of mitochondria-fueled NKA leading to intracellular Na⁺ loading [11], which in turn increases glycolysis-fueled NKA activity.

Note the similar magnitude of alkaline pHe shifts induced by 0-K⁺ [Fig. 1], iodoacetate [Fig. 3], and glucoprivation [Fig. 4] recorded during the day and at night. The results may be taken to suggest that the levels of proton production associated with glycolytic metabolism and activation of Na⁺ pumping activity may be similar between the day and night in the SCN. Along the same line of thinking, the similar magnitude of cyanide-induced acid shifts between the day and night [Fig. 2] suggests that mitochondrial inhibition may induce similar levels of proton production associated with enhanced glycolytic metabolism and activation of Na⁺ pumping activity. Nevertheless, the pHe is regulated by the pH buffering properties of extracellular fluid and the transmembrane flux of acid equivalents [17]. A better and more complete account of the similar day–night changes in the pHe related to energy metabolism, glucose utilization, and Na⁺ pumping activity require better understanding of, at least, the acid extruders responsible for the extracellular acidification associated with glycolysis-fueled NKA Na⁺ pumping activity.

Differential glucose sensitivity and utilization between oxidative and non-oxidative glycolytic pathways

One important observation is the differential inhibition by glucoprivation of cyanide-induced acidification and 0-K^+ -induced alkalization. Specifically, the cyanide-induced acidification could be completely abolished after glucose withdrawal for as short as ~30 min [Fig. 5A]. Since cyanide-induced acidification is associated with glycolytic metabolism [Fig. 3C], the result indicates the requirement for exogenous glucose to support glycolytic flux along the mitochondria-associated, oxidative glycolytic pathway. On the other hand, 0-K^+ -induced alkalization was only partially inhibited (by 33%) after glucose withdrawal for up to 30–60 min [Fig. 4B]. Since 0-K^+ -induced alkalization is associated with the blockade of glycolysis-fueled NKA Na^+ pumping activity [Fig. 3B], the result suggests the continuing glycolytic flux along the non-oxidative glycolytic pathway to power glycolysis-fueled NKA Na^+ pumping activity in spite of the lack of exogenous glucose. Importantly, there remains the standing acidification and 0-K^+ -induced alkalization, albeit to smaller extents, after prolonged glucose withdrawal for 6–9 h [Fig. 4C]. The results suggest the presence of energy reserve to continue supporting glycolytic flux along the non-oxidative glycolytic pathway, at least, to power glycolysis-fueled NKA Na^+ pumping activity.

Consistent with the idea of requirement for exogenous glucose to support glycolytic flux along the mitochondria-associated, oxidative glycolytic pathway, hypoglycemia (0.5 mM glucose) significantly inhibits cyanide-induced acidification without much effect on 0-K^+ -induced alkalization [Fig. 6]. In other words, the mitochondria-associated oxidative, as opposed to the non-oxidative, glycolytic pathway is susceptible to glucose shortage. Taken altogether, our results indicate differences in glucose sensitivity and utilization between oxidative and non-oxidative glycolytic pathways in the SCN. The mitochondria-associated, oxidative glycolytic pathway relies on the supply of exogenous glucose and is thus sensitive to glucose shortage. In contrast, the non-oxidative glycolytic pathway could use energy reserve, presumably glycogen, to support glycolytic metabolism, at least to power glycolysis-fueled NKA Na^+ pumping, and is thus relatively insensitive to glucose shortage. In this context, the glycolysis-fueled NKA appears to play a particularly important role at times of glucose shortage.

Implications for metabolic rhythms in the SCN

As stated in Introduction, the SCN clock exhibits diurnal rhythms in 2-deoxyglucose uptake, cytochrome oxidase activity, and NKA activity. The diurnal increase in SCN 2-deoxyglucose uptake (glucose utilization) is mostly eliminated by TTX, revealing a TTX-independent increase in the early morning, and is markedly suppressed by high Mg^{2+} solution that is known to block synaptic transmission [4]. Although the 2-deoxyglucose method cannot distinguish oxidative from non-oxidative glycolytic pathway, evidence indicates that oxidative phosphorylation produces most of the

ATP to power synaptic transmission in the brain [27]. Together with our finding of differential glucose sensitivity and utilization between oxidative and non-oxidative glycolytic pathways, a parsimonious model for the metabolic rhythms in the SCN suggests a diurnal increase in glucose uptake along the mitochondria-associated, oxidative glycolytic pathway to meet high energy demand for mitochondria-fueled NKA Na^+ pumping activity.

In addition to diurnal rhythms in metabolic activity, the SCN also exhibits diurnal rhythms in electrical activity and $[\text{Ca}^{2+}]_i$, with higher daytime spontaneous firing rate [28–31], $[\text{Ca}^{2+}]_i$ [32–34], and $\text{Na}^+/\text{Ca}^{2+}$ -exchanger activity [22]. Newman et al. [4] identifies three components of glucose utilization in SCN slices, with the largest component expressed during the day when the rate of TTX-sensitive neuronal firing is high, suggesting a coupling of glucose utilization to firing activity. Such coupling of energy metabolism to electrical activity has been shown to be mediated by activation of ouabain-sensitive Na^+ pumping activity in rat posterior pituitary [35]. The same might also occur in the rat SCN, as its NKA Na^+ pumping activity is regulated by intracellular Na^+ and energy metabolism [11]. In other words, NKA, via its energy-demanding nature and activation by intracellular Na^+ , should effectively couple elevated energy metabolism to higher daytime firing activity.

As to the TTX-resistant increase in glucose utilization in the early morning [4], our recent findings suggest a possible role of $[\text{Ca}^{2+}]_i$ along with NKA and mitochondria in such regulation. First, both $\text{Na}^+/\text{Ca}^{2+}$ -exchanger NCX1 and mitochondria play a role in regulating depolarization-evoked Ca^{2+} rise [22]. Second, NCX1 extrudes Ca^{2+} entering both the nimodipine-sensitive and -insensitive Ca^{2+} channels, whereas mitochondria preferentially buffers Ca^{2+} entering nimodipine-insensitive Ca^{2+} channels [36]. Third, TTX reduced only ~1/3 of basal Ca^{2+} influx and there remained ~1/4 of basal Ca^{2+} influx insensitive to combined presence of TTX and nimodipine [36]. As Ca^{2+} entering mitochondria could activate dehydrogenase to increase oxidative phosphorylation [37], it is possible that nimodipine-insensitive influx of Ca^{2+} may enter mitochondria to increase energy metabolism and thus glucose uptake.

Furthermore, NKA also plays an important role in the regulation of $[\text{Ca}^{2+}]_i$, in particular, associated with nimodipine-insensitive Ca^{2+} channels in the rat SCN [12]. Our results suggest that NKA regulate $[\text{Ca}^{2+}]_i$ by two mechanisms. First, NKA, via controlling $[\text{Na}^+]_i$ and transmembrane Na^+ gradient, regulates the rate of Ca^{2+} extrusion via NCX1. In this context, the diurnal rhythm in both NKA and $\text{Na}^+/\text{Ca}^{2+}$ exchanger (NCX) activity [6,22] suggests a concerted action of NKA and NCX to help regulate the diurnal increase in $[\text{Ca}^{2+}]_i$. Second, NKA, via controlling $[\text{Na}^+]_i$, may also regulate mitochondrial Ca^{2+} buffering, likely by acting on the mitochondrial $\text{Na}^+/\text{Ca}^{2+}$ -exchanger NCXL. Taken altogether, the results suggest that daytime increase in firing activity and $[\text{Ca}^{2+}]_i$ can enhance energy metabolism, either directly due to enhanced mitochondrial respiration as a result of mitochondrial Ca^{2+} uptake, or indirectly due to enhanced NKA activity as a result of Na^+ loading from neuronal firing and NCX activity.

Implications for metabolic regulation and glucose-sensing role of the SCN

The reliance on exogenous glucose of the mitochondria-associated glycolytic pathway suggests a locus of regulation by cellular activity and glucose availability. On the one hand, both light and glutamate increase 2-deoxyglucose uptake at night when light-induced phase shifts occur [3,38]. As glutamate-induced phase shifts at night involve both nimodipine-sensitive and -insensitive Ca^{2+} channels [39], Ca^{2+} entry via the nimodipine-insensitive Ca^{2+} channels could enter mitochondria to increase oxidative phosphorylation and thus the mitochondria-associated glycolytic flux [36]. Alternatively, glutamate-induced Na^+ loading might enhance NKA activity to increase energy metabolism and glucose uptake.

On the other hand, insulin- or fasting-induced hypoglycemia attenuates phase shifts induced by light at night in mice [8]. Our finding of selective attenuation of mitochondria-associated glycolysis by hypoglycemia (this study) suggests that hypoglycemia might compromise mitochondria to inhibit light-induced glutamatergic signaling.

Along the same line of thinking, hypoglycemia could compromise mitochondria to alter membrane excitability by influencing mitochondria-fueled NKA and ATP-sensitive K_t channels (K_{ATP} channels) [11]. Indeed, we recently demonstrated a selective activation of K_{ATP} channels by hypoglycemia in the rat K_{ATP} -expressing, vasopressin-containing SCN neurons [9]. The opening of K_{ATP} channels by cyanide or glucose shortage suggests the requirement of exogenous glucose for mitochondria-derived ATP to silence K_{ATP} channels in the rat SCN neurons. In this context, K_{ATP} plays a glucose-sensing role in the coupling of reduced excitability to glucose shortage in the rat SCN. Theoretically, mitochondria-fueled NKA should also be sensitive to glucose shortage. The ratiometric Na^+ imaging results indeed showed a mild increase of $[\text{Na}^+]_i$ by hypoglycemia (RC Cheng and RC Huang, unpublished observations). Further work is needed to better determine a glucose-sensing role of mitochondria-fueled NKA in the SCN neurons.

Last, as stated above, the glycolysis-fueled NKA appears to play a particularly important role at times of glucose shortage. The result of cyanide enhancement of O-K^+ -induced alkalization [Fig. 2B] suggests that glycolysis-fueled NKA activity could be augmented by cyanide inhibition of mitochondrial respiration, most likely as a result of cyanide-induced loading of intracellular Na^+ [11]. In other words, at times of glucose shortage that compromises mitochondria-fueled NKA, the glycolysis-fueled NKA activity might be enhanced to help better regulate homeostasis of intracellular Na^+ and Ca^{2+} as well as extracellular K^+ .

Conclusion

In conclusion, glycolytic metabolism and activation of Na^+ pumping contributes to the standing acidification in the rat SCN. Furthermore, the oxidative and non-oxidative glycolytic pathways differ in their glucose sensitivity and utilization.

The mitochondria-associated, oxidative glycolytic pathway is susceptible to glucose shortage and plays a role in metabolic regulation of the circadian clock. In contrast, the non-oxidative glycolytic pathway is relatively insensitive to glucose shortage and could maintain Na^+ pumping activity to help better regulate ion homeostasis at times of metabolic stress such as glucose shortage.

Funding

This work was supported by Chang Gung Medical Foundation (CMRPD1H0072 and CMRPD1H0073; R.C.H) and by Taiwan Ministry of Science and Technology (MOST108-2320-B-182-017-MY3; R.C.H).

Conflicts of interest

The authors declare no conflicts of interest.

Acknowledgements

We are grateful to Neuroscience Research Center of Chang Gung Memorial Hospital, Linkou Medical Center, Taiwan.

REFERENCES

- [1] Green CB, Takahashi JS, Bass J. The meter of metabolism. *Cell* 2008;134:728–42.
- [2] Dibner C, Schibler U, Albrecht U. The mammalian circadian timing system: organization and coordination of central and peripheral clocks. *Annu Rev Physiol* 2010;72:517–49.
- [3] Schwartz WJ, Gainer H. Suprachiasmatic nucleus: use of ^{14}C -labeled deoxyglucose uptake as a functional marker. *Science* 1977;197:1089–91.
- [4] Newman GC, Hospod FE, Patlak CS, Moore RY. Analysis of in vitro glucose utilization in a circadian pacemaker model. *J Neurosci* 1992;12:2015–21.
- [5] López L, Lorente L, Arias J, González-Pardo H, Cimadevilla J, Arias JL. Changes of cytochrome oxidase activity in rat suprachiasmatic nucleus. *Brain Res* 1997;769:367–71.
- [6] Wang HY, Huang RC. Diurnal modulation of the Na^+/K^+ -ATPase and spontaneous firing in the rat retinorecipient clock neurons. *J Neurophysiol* 2004;92:2295–301.
- [7] Challet E. Interactions between light, mealtime and calorie restriction to control daily timing in mammals. *J Comp Physiol B* 2010;180:631–44.
- [8] Challet E, Losee-Olson S, Turek FW. Reduced glucose availability attenuates circadian responses to light in mice. *Am J Physiol* 1999;276:R1063–70.
- [9] Yang JJ, Cheng RC, Cheng PC, Wang YC, Huang RC. K_{ATP} channels mediate differential metabolic responses to glucose shortage of the dorsomedial and ventrolateral oscillators in the central clock. *Sci Rep* 2017;7:640.
- [10] Wang YC, Huang RC. Effects of sodium pump activity on spontaneous firing in neurons of the rat suprachiasmatic nucleus. *J Neurophysiol* 2006;96:109–18.
- [11] Wang YC, Yang JJ, Huang RC. Intracellular Na^+ and metabolic modulation of Na/K pump and excitability in the rat

- suprachiasmatic nucleus neurons. *J Neurophysiol* 2012;108:2024–32.
- [12] Cheng RC, Cheng PC, Wang YC, Huang RC. Role of intracellular Na^+ in the regulation of $[\text{Ca}^{2+}]_i$ in the rat suprachiasmatic nucleus neurons. *Int J Mol Sci* 2019;20:4868.
- [13] Wong-Riley MTT. Cytochrome oxidase: an endogenous metabolic marker for neuronal activity. *Trends Neurosci* 1989;12:94–101.
- [14] Erecińska M, Dagani F. Relationships between the neuronal sodium/potassium pump and energy metabolism: effects of K^+ , Na^+ and adenosine triphosphate in isolated brain synaptosomes. *J Gen Physiol* 1990;95:591–616.
- [15] Erecińska M, Silver IA. ATP and brain function. *J Cerebr Blood Flow Metabol* 1989;9:2–19.
- [16] Robergs RA, Ghasvand F, Parker D. Biochemistry of exercise-induced metabolic acidosis. *Am J Physiol Regul Integr Comp Physiol* 2004;287:R502–16.
- [17] Chesler M. Regulation and modulation of pH in the brain. *Physiol Rev* 2003;83:1183–221.
- [18] Cheng PC, Lin HY, Chen YS, Cheng RC, Su HC, Huang RC. The Na^+/H^+ -exchanger NHE1 regulates extra- and intracellular pH and nimodipine-sensitive $[\text{Ca}^{2+}]_i$ in the suprachiasmatic nucleus. *Sci Rep* 2019;9:6430.
- [19] Tong CK, Brion LP, Suarez C, Chesler M. Interstitial carbonic anhydrase (CA) activity in brain is attributable to membrane-bound CA type IV. *J Neurosci* 2000;20:8247–53.
- [20] Dmitriev AV, Mangel SC. Circadian clock regulation of pH in the rabbit retina. *J Neurosci* 2001;21:2897–902.
- [21] Deveau JST, Lindinger MI, Grodzinski B. An improved method for constructing and selectively silanizing double-barreled, neutral liquid-carrier, ion-selective microelectrodes. *Biol Proc* 2005;7:31–40.
- [22] Wang YC, Chen YS, Cheng RC, Huang RC. Role of $\text{Na}^+/\text{Ca}^{2+}$ exchanger in Ca^{2+} homeostasis in the rat suprachiasmatic nucleus neurons. *J Neurophysiol* 2015;113:2114–26.
- [23] Romero MF, Fulton CM, Boron WF. The SLC4 family of HCO_3^- transporters. *Pflugers Arch – Eur J Physiol* 2004;447:495–509.
- [24] Allen DG, Morris PG, Orchard CH, Pirolo JS. A nuclear magnetic resonance study of metabolism in the ferret heart during hypoxia and inhibition of glycolysis. *J Physiol* 1985;361:185–204.
- [25] Bountra C, Kaila K, Vaughan-Jones RD. Mechanism of rate-dependent pH changes in the sheep cardiac Purkinje fibre. *J Physiol* 1988;406:483–501.
- [26] Wu ML, Vaughan-Jones RD. Effect of metabolic inhibitions and second messengers upon Na^+/H^+ exchange in the sheep cardiac Purkinje fibre. *J Physiol* 1994;478:301–13.
- [27] Harris JJ, Jolivet R, Attwell D. Synaptic energy use and supply. *Neuron* 2012;75:762–77.
- [28] Inouye SIT, Kawamura H. Persistence of circadian rhythmicity in a mammalian hypothalamic 'island' containing the suprachiasmatic nucleus. *Proc Natl Acad Sci USA* 1979;76:5962–6.
- [29] Green DJ, Gillette R. Circadian rhythm of firing rate recorded from single cells in the rat suprachiasmatic brain slice. *Brain Res* 1982;245:198–200.
- [30] Groos GA, Hendriks J. Circadian rhythms in electrical discharge of rat suprachiasmatic neurones recorded in vitro. *Neurosci Lett* 1982;34:283–8.
- [31] Shibata S, Oomura Y, Kita H, Hattori K. Circadian rhythmic changes of neuronal activity in the suprachiasmatic nucleus of the rat hypothalamic slice. *Brain Res* 1982;247:154–8.
- [32] Colwell CS. Circadian modulation of calcium levels in cells in the suprachiasmatic nucleus. *Eur J Neurosci* 2000;12:571–6.
- [33] Ikeda M, Sugiyama T, Wallace CS, Gompf HS, Yoshioka T, Miyawaki A, et al. Circadian dynamics of cytosolic and nuclear Ca^{2+} in single suprachiasmatic nucleus neurons. *Neuron* 2003;38:253–63.
- [34] Enoki R, Huroda S, Ono D, Hasan MT, Ueda T, Honma S, et al. Topological specificity and hierarchical network of the circadian calcium rhythm in the suprachiasmatic nucleus. *Proc Natl Acad Sci USA* 2012;109:21498–503.
- [35] Mata M, Fink DJ, Gainer H, Smith CB, Davidsen L, Savaki H, et al. Activity-dependent energy metabolism in rat posterior pituitary primarily reflects sodium pump activity. *J Neurochem* 1980;34:213–5.
- [36] Cheng PC, Wang YC, Chen YS, Cheng RC, Yang JJ, Huang RC. Differential regulation of nimodipine-sensitive and -insensitive Ca^{2+} influx by the $\text{Na}^+/\text{Ca}^{2+}$ exchanger and mitochondria in the rat suprachiasmatic nucleus neurons. *J Biomed Sci* 2018;25:44.
- [37] Rizzuto R, De Stefani D, Raffaello A, Mammucari C. Mitochondria as sensors and regulators of calcium signalling. *Nat Rev Mol Cell Biol* 2012;13:566–78.
- [38] Shibata S, Tominaga K, Hamada T, Watanabe S. Excitatory effect of N-methyl-D-aspartate and kainate receptor on the 2-deoxyglucose uptake in the rat suprachiasmatic nucleus in vitro. *Neurosci Lett* 1992;139:83–6.
- [39] Kim DY, Choi HJ, Kim JS, Kim YS, Jeong DU, Shin HC, et al. Voltage-gated calcium channels play crucial roles in the glutamate-induced phase shifts of the rat suprachiasmatic circadian clock. *Eur J Neurosci* 2005;21:1215–22.